HHS Public Access

Author manuscript

Psychopharmacology (Berl). Author manuscript; available in PMC 2020 March 01.

Published in final edited form as:

Psychopharmacology (Berl). 2019 March ; 236(3): 939–952. doi:10.1007/s00213-018-5059-5.

Structure-activity relationships of bath salt components: substituted cathinones and benzofurans at biogenic amine transporters

Amy J Eshleman[1,2], **Shanthi Nagarajan**[3], **Katherine M Wolfrum**[1], **John F Reed**[1], **Tracy L Swanson**[1,2], **Aaron Nilsen**[1,3], and **Aaron Janowsky**[1,2,4]

[1]Research Service, VA Portland Health Care System

[2]Departments of Behavioral Neuroscience and Psychiatry (AJE, AJ)

[3]Medicinal Chemistry Core (SN, AN)

[4]The Methamphetamine Abuse Research Center (AJ), Oregon Health & Science University, Portland OR, 97239, United States

Abstract

Rationale—New psychoactive substances (NPS), including substituted cathinones and other stimulants, are synthesized, sold on the Internet, and ingested without knowledge of their pharmacological activity and/or toxicity. *In vitro* pharmacology plays a role in therapeutic drug development, drug-protein *in silico* interaction modeling, and drug scheduling.

Objectives—The goal of this research was to determine mechanisms of action that may indicate NPS abuse liability.

Methods—Affinities to displace the radioligand [^{125}I]RTI-55 and potencies to inhibit [^{3}H]neurotransmitter uptake for 22 cathinones, 6 benzofurans and another stimulant were characterized using human embryonic kidney cells stably expressing recombinant human transporters for dopamine, norepinephrine or serotonin (hDAT, hNET, or hSERT, respectively). Selected compounds were tested for potencies and efficacies at inducing [^{3}H]neurotransmitter release *via* the transporters. Computational modeling was conducted to explain plausible molecular interactions established by NPS and transporters.

Results—Most α-pyrrolidinophenones had high hDAT potencies and selectivities in uptake assays, with hDAT/hSERT uptake selectivity ratios of 83 −360. Other substituted cathinones varied in their potencies and selectivities, with *N*-ethyl-hexedrone and *N*-ethyl-pentylone having highest hDAT potencies and *N*-propyl-pentedrone having highest hDAT selectivity. 4-Cl-

Corresponding author Amy J. Eshleman, Ph.D., Research Service (R&D22), VA Portland Health Care System, 3710 SW US Veterans Hospital Rd., Portland OR. USA, Tel: (503)-220-8262 ×57484, Fax: (503)-721-7839, eshleman@ohsu.edu.

Authorship contributions:

Participated in research design: Eshleman, Janowsky, Nagarajan, Nilsen

Conducted experiments: Eshleman, Wolfrum, Reed, Swanson

Performed data analysis: Eshleman, Wolfrum, Reed, Swanson, Nagarajan

Wrote or contributed to the writing of the manuscript: Eshleman, Janowsky, Nagarajan, Nilsen

Conflict of interest

All authors declare that they have no conflicts of interest.

ethcathinone and 3,4-methylenedioxy-*N*-propylcathinone had higher hSERT selectivity. Benzofurans generally had low hDAT selectivity, especially 5-MAPDB, with 25-fold higher hSERT potency. Consistent with this selectivity, the benzofurans were releasers at hSERT. Modeling indicated key amino acids in the transporters' binding pockets that influence drug affinities.

Conclusions—The α-pyrrolidinophenones, with high hDAT selectivity, have high abuse potential. Lower hDAT selectivity among benzofurans suggests similarity to MDMA, entactogens with lower stimulant activity.

Keywords

New psychoactive substances; psychostimulant; pharmacology; transporter; benzofurans; cathinones

Introduction

Novel stimulants, a class of new psychoactive substances which includes amphetamine-related compounds, substituted cathinones and benzofurans, are being detected in "street drug" combinations (bath salts), in blood and/or tissue of emergency room patients, and in stimulant-abuse related deaths (King and Corkery 2018; Krotulski et al. 2018; Tettey et al. 2018; Simmler and Liechti 2018). The reported use or detection of new compounds includes mexedrone, PV9 (αPOP) and 2-MAPB (Roberts et al. 2017; Uchiyama et al. 2014; Staeheli et al. 2017). *In vitro* pharmacological assays are valuable for determining the initial sites of action of new compounds, and can aid in predicting abuse potential and possible toxicity by comparison with well characterized compounds (Simmler and Liechti 2017).

Synthetic cathinones (SC), with a keto group on the *beta* carbon, and abused amphetamines, target the DAT, SERT and NET and have abuse potential (Dal Cason et al. 1997; De Felice et al. 2014; Glennon and Dukat 2017). Acute toxicity is associated with sympathomimetic effects, including hyperthermia, hypertension, tachycardia and anxiety (Tyrkko et al. 2016). In addition, some SCs are structurally similar to MDMA, an entactogen. While entactogens are associated with feelings of well-being and empathy, they can increase the risk of developing life-threatening serotonin (5-HT) syndrome (de la Torre et al. 2004).

Several generations of SC have been detected in online drug supply offerings. The first wave included MDPV, a very potent uptake blocker, and methylone, a substrate that increases extracellular neurotransmitter concentrations both by competing for reuptake *via* the transporters and by inducing neurotransmitter release from intracellular stores (Eshleman et al. 2013; Baumann et al. 2013; Schindler et al. 2016; Hadlock et al. 2011; Lopez-Arnau et al. 2012; Cameron et al. 2013; Iversen et al. 2013). A second generation included α-PVP, pentedrone and pentylone (Simmler et al. 2014; Eshleman et al. 2017; Gatch et al. 2015; Saha et al. 2015). Many first and second generation SCs are Schedule 1 substances in the USA, having no therapeutic uses and high potential for abuse (Drug Enforcement Administration 2011; Drug Enforcement Administration 2017). We now describe another generation of SCs, frequently created by adding a halogen, methyl or other small moiety to

previously characterized and controlled compounds to circumvent regulatory scheduling (Fig 1).

Pyrrolidino-substituted cathinones have a 5-membered nitrogen-containing ring on the *alpha* carbon (Fig 1A) and are generally pure uptake blockers with no releasing activity (Eshleman et al. 2013; Eshleman et al. 2017; Marusich et al. 2014; Rickli et al. 2015a). In addition, the carbon chain length on the alpha carbon affects DAT affinity and potency, with compounds containing tails with 3–6 carbons having very high affinity (Kolanos et al. 2015; Eshleman et al. 2017).

There is limited information about the mechanism of action and toxicity of newer synthetic cathinones. In synaptosomes, dimethylone (bk-MDDMA) inhibits uptake by DAT, SERT and NET with micromolar potencies, has minimal effect on neurotransmitter release from DAT and NET, and very low potency at inducing release *via* SERT (Sandtner et al. 2016). In rat brain synaptosomes, mexedrone is a weak non-selective uptake blocker with no releasing activity at DAT and NET, but is a low potency releaser at SERT (McLaughlin et al. 2017). 4-F-α-PVP was synthesized by Meltzer et al. (2006) in an effort to find medications for cocaine abuse.

Benzofurans, structurally similar to MDMA, have similar or higher potency at inhibition of 5-HT uptake in rat synaptosomes than 3,4-methylenedioxyamphetamine (Monte et al. 1993). Microdialysis in mouse striatum reveals that 2-MAPB and 5-MAPB increase 5-HT levels more than dopamine (DA) levels (Fuwa et al. 2016). 6-APB (Benzofury) and 5-MAPDB inhibit NET and SERT uptake more than DAT uptake (Rickli et al. 2015b). At micromolar concentrations, some benzofurans interact with nicotinic, adrenergic and 5-$HT2_{A,B,C}$ receptors (Shimshoni et al. 2017). The benzofurans, consumed as stimulating or entactogenic drugs, have adverse effects typical for stimulants (Welter-Luedeke and Maurer 2016; Hofer et al. 2017).

The goal of this research was to determine mechanisms of action of these compounds that may indicate abuse liability. We characterized *in vitro* pharmacology of 8 pyrrolidino cathinones, 6 pentedrone and 5 pentylone analogs, 6 benzofurans, and 3 additional cathinones. *In silico* modeling revealed specific amino acids in the transporters that affected affinity of compounds. For a subset of compounds, we determined potential to induce release of [^{3}H]neurotransmitter from cells. Using uptake inhibitory potencies, we determined selectivity ratios for potency at DAT vs SERT, which aids in prediction of abuse potential (Baumann et al. 2012).

Methods

Drugs and Materials

Cocaine, methamphetamine (METH), MDMA, and methcathinone (MCAT) were generously supplied by the NIDA Drug Supply Program (Bethesda, MD). The hydrochloride salts of 4'-chloro-α-pyrrolidinopropiophenone (4-Cl-α-PPP); 4-fluoro-α–pyrrolidinopentiophenone (4-F-α-PVP); 4'-chloro-α–pyrrolidinopentiophenone (4-Cl-α-PVP); 3',4'-tetramethylene-α-pyrrolidinovalerophenone (TH-PVP); 4'-fluoro-α–

pyrrolidinohexanophenone (4-F-α-PHP); 4'-methyl-α–pyrrolidinohexanophenone (4-Me-α-PHP); 3,4-methylenedioxy-α–pyrrolidinohexanophenone (3,4-MDPHP); 1-phenyl-2-(pyrrolidin-1-yl)octan-1-one (PV9); 4-chloro pentedrone (4-CPD); 4-methyl pentedrone (4-MPD); α-ethylaminopentiophenone (α-EPP); α-propylaminopentiophenone (*N*-propylpentedrone); 4-methyl-α-ethylaminopentiophenone (4-MEAP); α-ethylaminohexanophenone (*N*-Et Hexedrone); *N*-ethyl pentylone; 3,4-methylenedioxy-*N*-propylcathinone (PRONE); bk-MDDMA (dimethylone); bk-DMBDB (dibutylone); *N,N*-dimethylpentylone (bk-DMBDP); 3-methoxy-2-(methylamino)-1-(*p*-tolyl)propan-1-one (mexedrone); 4-Cl-ethcathinone (4-CEC); 3-methylmethcathinone (3-MMC); 1-[1-(phenylmethyl)butyl]-pyrrolidine (Prolintane); *N*,α-dimethyl-2-benzofuranethanamine (2-MAPB); *N*,α-dimethyl-5-benzofuranethanamine (5-MAPB); *N*,α-dimethyl-6-benzofuranethanamine (6-MAPB); 1-(2,3-dihydrobenzofuran-5-yl)-*N*-methylpropan-2-amine (5-MAPDB); α-methyl-6-benzofuranethanamine (6-APB); and *N*-ethyl-α-methyl-6-benzofuranethanamine (6-EAPB) were purchased from Cayman Chemical (Ann Arbor, MI). [^{125}I]RTI-55, [^{3}H]DA, [^{3}H]5-HT, and [^{3}H]norepinephrine (NE), were purchased from Perkin Elmer Life & Analytical Sciences (Boston, MA). Drugs were dissolved in DMSO to make a 10 or 100 mM stock. FetalClone and bovine calf serum (BCS) were purchased from ThermoFisher, Waltham, MA. Other chemicals were purchased from Sigma-Aldrich (St. Louis, MO).

Inhibition of [^{125}I]RTI-55 binding to, and [^{3}H]neurotransmitter uptake by, hDAT, hSERT or hNET expressed in HEK-293 Cells

RTI-55 is a stable cocaine homolog (a phenyltropane-derived psychostimulant) and DAT inhibitor that binds to the three transporters with low nM affinity. The methods for characterizing radioligand binding and functional uptake assays have been described (Eshleman et al. 1999). Human embryonic kidney (HEK-293) cells stably expressing the recombinant hDAT (HEK-hDAT), hSERT (HEK-hSERT) or hNET (HEK-hNET) were used. Cells were cultured in DMEM supplemented with 5% FetalClone, 5% bovine calf serum, penicillin/streptomycin and 2 μg/ml puromycin (hDAT and hSERT) or 10% FetalClone, penicillin/streptomycin and 300 μg/ml G418. (hNET). For [^{125}I]RTI-55 competition binding assays, a total particulate membrane preparation was used, resuspended in 50, 15 or 5 ml (hDAT, hSERT, or hNET, respectively) of 0.32 M sucrose /cell culture plate.

Binding assay conditions: Each assay well contained membrane preparation, test compound or buffer (Krebs-HEPES, pH 7.4; 122 mM NaCl, 2.5 mM $CaCl_2$, 1.2 mM $MgSO_4$, 10 μM pargyline, 100 μM tropolone, 0.2% glucose and 0.02% ascorbic acid, buffered with 25 mM HEPES), and [^{125}I]RTI-55 (40–80 pM final concentration) in a final volume of 250 μl. Radioligand was added after a 10 min preincubation of membranes with test compounds. Binding was terminated after 90 min incubation by filtration over Filtermat A filters (Perkin Elmer) using a Tomtec 96-well cell harvester (Hamden, CT). Radioactivity on the filter was determined using a Perkin Elmer μbeta-plate reader. Specific binding was defined as the difference in binding observed in the presence and absence of 5 μM mazindol (hDAT and hNET) or 5 μM imipramine (hSERT).

For [^{3}H]neurotransmitter uptake assays, confluent cells were removed from plates by gentle scraping and trituration with a pipette. Krebs-HEPES and test compound, compound used to define non-specific uptake (5 μM mazindol (hDAT and hNET) or 5 μM imipramine (hSERT)) or buffer and cells were added to vials and preincubated for 10 min at 25°C. [^{3}H]DA (hDAT), [^{3}H]5-HT (hSERT), or [^{3}H]NE (hNET) (20 nM final concentration) was added and uptake was conducted for 10 min. Uptake was terminated by filtration as described above through Filtermat A filters presoaked in 0.05% polyethylenimine.

Biogenic amine transporters: [^{3}H]Neurotransmitter release

Cells were scraped from one plate (hDAT and hSERT) or three plates (hNET) into 8 ml Krebs HEPES buffer, centrifuged at 500 rpm for 7 min, and resuspended in 8 ml Krebs HEPES (Gatch et al., 2011; Eshleman et al., 2013). Cells were loaded for 15 min at 30°C with 120 nM [^{3}H]DA (hDAT), 30 min at 25°C with 20 nM [^{3}H]5-HT (hSERT) or 12 min at 30°C with 120 nM [^{3}H]NE (hNET). After centrifugation to remove extracellular [^{3}H]neurotransmitter, cells were resuspended in Krebs HEPES, and cell suspension (280 μl) was added to a Suprafusion 2500 device (Brandel, Gaithersburg, MD) using polyethylene discs in reaction tubes. Drug-induced neurotransmitter release was conducted at 30°C (hDAT) or 25°C (hSERT and hNET). Baseline release was established by perfusion of buffer (12 min hDAT and hSERT or 15 min hNET), with the last 6 min (3 × 2 min fractions) collected. Drug-induced release was initiated by perfusion of drug solutions (10 nM to 100 μM) for 22 min, collecting 11 × 2 min fractions. Maximal release typically occurred 4–6 min after substrate perfusion. To lyse cells and release remaining radioactivity, SDS (1%) was perfused, and 4 × 2.5 min fractions were collected. Radioactivity in the samples was determined using conventional liquid scintillation spectrometry. An advantage of this method is continuous removal of released [^{3}H]neurotransmitter, decreasing reuptake of released [^{3}H]neurotransmitter, which could be a confound. In addition, the use of transfected cells stably expressing a single transporter allows the release to be conducted in the absence of inhibitors for other transporters, as is needed with release assays conducted with synaptosomes.

Modeling of bath salts' interaction with the transporters

The crystal structures for hDAT and hNET are not available, therefore we used homology modeling method to generate 3D models based on the available hSERT crystal structure (Coleman et al., 2016; PDB: 5I6X) as a template. The sequence identity of the aligned regions of the template and target sequence is 51.4% (hDAT) and 53.4% (hNET). The sequence alignment and the template crystal structure served as an input to MODELLER 9.14 program (Sali and Blundell, 1993; Webb and Sali, 2017) with the best models selected based on the discrete optimized protein energy (DOPE) score (Shen and Sali, 2006) and visualization.

To model ligand/protein interactions, we used the Schrödinger Small Molecule Drug Discovery Suite of Programs (Schrödinger, LLC, New York, NY, 2013). The crystal structure of hSERT and homology models generated for hDAT and hNET were subjected to docking. Before docking all ligand molecules were aligned using paroxetine as a template, key pharmacophores were generated based on the alignment and matching atom types. All

ligands carry a positive net charge (+1) due to a protonated nitrogen (Fig 1). The induced-fit docking (IFD) protocol (Sherman et al., 2006) was performed in extended mode; the active-site was defined based on the 20Å surrounding the conserved aspartate. During IFD, protein residues within 5Å of the protein active site surrounding the docked pose were allowed to move. Under physiological conditions both protein and ligand molecules are flexible; IFD mimics this flexibility while docking. The binding poses were rank-ordered using the grid-based ligand docking with energetics (GLIDE) scoring function (Friesner et al., 2004; Friesner et al., 2006; Halgren et al., 2004).

Data analysis

Competition binding data were normalized to specific binding in the absence of drug. Three or more independent competition experiments were conducted with duplicate determinations. Data was analyzed with GraphPAD Prism7 (La Jolla, CA), and IC_{50} values were converted to K_i values using the Cheng-Prusoff equation (Cheng and Prusoff, 1973) using K_d values previously determined (Eshleman et al., 2013). Differences in affinities were assessed by one-way ANOVA using the logarithms of K_i values and Dunnett's multiple comparison test compared test compounds to a drug standard as noted. In uptake assays, IC_{50} values were determined using Prism7. The DAT/SERT ratio was determined by dividing 1/(DAT IC_{50}) by 1/(SERT IC_{50}), with higher values indicating more DAT selectivity (Baumann et al. 2012).

For release assays, fractional release was defined as radioactivity in a fraction divided by the total radioactivity remaining in cells. The area under the curve (AUC) for each time course was calculated using Prism7 with baseline defined as the average of the two lowest fractions. For each experiment, the basal release AUC in the absence of drug was subtracted from each AUC before normalizing to the percent of maximal METH-stimulated release. Prism7 was used to calculate EC_{50} values using sigmoidal nonlinear regression.

Results

α-Pyrrolidinophenones at hDAT, hSERT and hNET: Inhibition of [^{125}I]RTI-55 binding and [^{3}H]neurotransmitter uptake and efficacy at inducing [^{3}H]neurotransmitter release

[^{125}I]RTI-55 binding and [^{3}H]neurotransmitter uptake: α-Pyrrolidinophenones are cathinones with a pyrrolidine group with varying carbon chain lengths on the α-carbon (Fig 1A). The prototypical α-pyrrolidinophenones, α-PVP, has a 3 carbon tail (Fig 1A, position R_2). All α-pyrrolidinophenones tested, except TH-PVP, had rank order of binding affinity of hDAT > hNET > hSERT, which suggests selectivity for catecholamine versus indoleamine transporters (Table 1). Five compounds had substitutions at the para position of the benzene ring (Fig 1A, R_1) and varied carbon tail length (Fig 1A, R_2): 4-Cl-α-PPP (1 carbon), 4-F-α-PVP and 4-Cl-α-PVP (3 carbons), and 4-F-α-PHP and 4-Me-α-PHP (4 carbons). 4-Me-α-PHP had highest hDAT affinity (23 nM) and 4-Cl-α-PVP had highest affinities for hSERT (2.02 μM) and hNET (281 nM, Table 1). TH-PVP, with a six-membered ring fused to the benzene ring of α-PVP, had higher affinity for hSERT than hDAT or hNET. Compared to α-PVP, 4-Cl-α-PVP, 4-F-α-PVP, 4-F-α-PHP and TH-PVP had decreased hDAT affinities

(*p*s<0.05–0.0001), while all had increased hSERT and decreased hNET affinities (ps<0.05–0.001).

In the uptake assays, among these compounds, 4-Cl-α-PPP, with the shortest carbon chain, had the lowest hDAT and hNET uptake inhibition potencies (0.73 and 1.42 μM, respectively), while 4-F-α-PVP had the lowest hSERT potency (42.5 μM, Fig 2A, Table 1). The potencies to inhibit uptake by hDAT and hNET were very similar for each compound, as shown for 4-F-α-PVP, 4-Cl-α-PVP and TH-PVP (Fig 2A,B,C). 4-Cl-α-PVP (Fig 2B), 4-F-α-PHP and 4-Me-α-PHP had very high potency at hDAT (13–38 nM), while 4-F-α-PVP had the highest selectivity for hDAT over hSERT (360 fold, Fig 2A). 3,4-MDPHP, which has a 3,4-methylenedioxy moiety and a 4-carbon tail (Fig 1A), had the highest hDAT potency of all α-pyrrolidinophenones tested (8.4 nM), and 160-fold hDAT selectivity (Table 1, Fig 2D). PV9, with a 7 carbon tail (Fig 1A), had similar potency as the substituted PVP and PHP compounds. No compound had significantly increased hDAT or hNET potency compared to α-PVP. 4-Cl-α-PPP, 4-F-α-PVP, TH-PVP and PV9 had lower potency at hDAT (ps<0.05–0.0001), and 4-Cl-α-PPP, 4-F-α-PVP, TH-PVP and 4-F-α-PHP had lower potency at hNET (ps<0.05–0.0001) compared to α-PVP. In contrast, at hSERT all compounds except 4-F-α-PVP had increased potency (ps<0.05–0.0001) compared to α-PVP. TH-PVP had the highest SERT potency (0.208 μM) and was the only compound in this set with selectivity for SERT over DAT (12-fold, Fig 2C). Prolintane, structurally similar to α-PVP except without the ketone group (Fig 1A) and thus not a substituted cathinone, had hDAT and hNET potencies similar to 4-F-α-PVP but 40-fold higher hSERT potency (p<0.0001, Table 1).

[^{3}H]Neurotransmitter Release: The pyrrolidino cathinone analogs TH-PVP and 4-Cl-PVP had minimal to no releasing efficacy at hDAT, hSERT or hNET (Table 2).

Other substituted cathinones at hDAT, hSERT and hNET: Inhibition of [^{125}I]RTI-55 binding and [^{3}H]Neurotransmitter uptake and release

Five pentedrone analogs (Fig 1B) with 3 carbon tails were tested. Two compounds, 4-MPD and 4-CPD, had para-methyl or -chloro addition to the phenyl ring (Fig 1B, R_1). Both substitutions decreased hDAT affinity approximately 4- to 5-fold (p<0.01) compared to pentedrone and increased hSERT affinity modestly. In uptake assays, these phenyl ring substitutions had less effect on hDAT potency; 4-CPD had lower potency (p<0.05) while 4-MPD had potency similar to pentedrone. However, potency was increased 15- to 17-fold at SERT (p<0.001), shifting the hDAT/hSERT selectivity from 50 for pentedrone to 1–3 for the para-substituted compounds. 4-CPD had similar potencies at hDAT, hSERT and hNET, (Fig 2E). α-EPP and *N*-propyl pentedrone have ethyl and propyl substitutions for the methyl group on the nitrogen (Fig 1B, R_2). The ethyl substitution increased hNET affinity (p<0.05) and had minimal effects on uptake inhibition potency by the transporters, with an overall effect of slightly increasing the hDAT/hSERT ratio (Fig 2F). The propyl substitution had little effect on hDAT or hNET affinity or potency, but decreased hSERT potency (p<0.001), thus increasing the hDAT/hSERT ratio compared to pentedrone (Fig 2G). 4-MEAP, with both a para-methyl group and an *N*-ethyl group (Fig 1B, $R_{1\&2}$), increased affinity 20-fold and potency 8-fold for hSERT compared to pentedrone (p<0.0001), decreasing hDAT selectivity 8-fold (Fig 2H). *N*-Et-hexedrone is similar to α-EPP but has a 4 carbon tail (Fig

1B, R_3). It has similar affinities for the transporters as α-EPP and slightly higher hDAT/hSERT selectivity (100).

Five compounds in this group have the 3,4 methylenedioxy moiety which is shared with MDMA (Fig 1C). Two analogs differ from pentylone by substitution of the methyl group on the nitrogen. *N*-Et pentylone has an ethyl group at this position (Fig 1C, R_2) and has similar hDAT affinity and higher hSERT ($p<0.0001$) and hNET ($p<0.01$) affinities compared to pentylone. However, increased hDAT potency ($p<0.01$) resulted in a ~2-fold increase in hDAT/hSERT selectivity (Table 1). bk-DMBDP has 2 methyl groups on the nitrogen (Fig 1C, $R_{1\&2}$) and increased hNET affinity ($p<0.01$) and decreased hSERT potency ($p<0.001$), which slightly shifted selectivity toward hDAT (Table 1). Dibutylone, which is similar to bk-DMBDP with two methyl groups on the nitrogen but with a shorter tail (Fig 1C, R_3), had hDAT and hNET affinities and potencies similar to pentylone and very low hSERT affinity and potency. The shorter carbon tail caused lower affinity and potency at all three transporters. Dimethylone, with 2 methyl groups on the nitrogen and a short 1 carbon tail (Fig 1C, R_3), had the lowest affinities and potencies of the pentylone group, with all parameters in the micromolar range (Table 1). PRONE, similar to dimethylone with a short 1 carbon tail but with a propyl group instead of the dimethyl groups (Fig 1C, $R_{2\&3}$), had very low affinities and potencies at all three transporters. In the release assays, three compounds, *N*-Et pentylone, dibutylone, and dimethylone, had no efficacy at inducing release from hDAT, hSERT or hNET (Table 2), consistent with previous results with pentylone (Eshleman et al. 2017).

Three MCAT analogs with modifications on the phenyl ring were tested (Fig 1D). MCAT had low micromolar affinities for hDAT and hNET, and much lower hSERT affinity. In uptake assays, MCAT had a rank order of potency of hNET > hDAT >>hSERT (Fig 2I). In release assays, MCAT had high nanomolar to low micromolar potency at NET and DAT, but had 50-fold lower potency at SERT (Table 2, Fig 3A). 3-MMC, with a meta-methyl on the phenyl ring (Fig 1, R_2), had similar hDAT affinity and potency as MCAT. In contrast, at hSERT it had ~40-fold higher affinity and 6.5-fold higher potency (ps<0.0001) than MCAT, resulting in a hDAT/hSERT shift from 130 for MCAT to 10 for 3-MMC (Table 1, Fig 2J). 4-CEC, with a para-chloro on the phenyl ring and an ethyl on the nitrogen (Fig 1, $R_{1\&3}$), had high nanomolar to micromolar hDAT and hNET affinities and potencies. At hSERT, it had low micromolar binding affinity and mid nanomolar uptake potency, resulting in a 3-fold selectivity for hSERT (Fig 2K). Consistent with this selectivity, 4-CEC had minimal releasing efficacy at hDAT and hNET, but had full releasing efficacy at hSERT, suggesting that it is a substrate only at the latter (Fig 3B). These results are similar to those reported earlier for ethylone (ethcathinone) (Eshleman et al. 2017). Mexedrone has a para methyl group and a methyl-methoxy tail on the alpha carbon (Fig 1, $R_{1\&4}$). It had low affinities and potencies at all transporters and low selectivity for hDAT (Table 1, Fig 2L). In release assays it had no hDAT efficacy, minimal hNET efficacy, but full efficacy with low potency at hSERT, suggesting that it too is a substrate only at hSERT (Fig 3C).

Benzofurans

2-MAPB was the only benzofuran with the furan group directly attached to the ethylamine group (Fig 1E). It had low micromolar affinities for hDAT, hSERT and hNET, and nanomolar uptake potency with rank order hNET>hDAT>hSERT (Table 1). 2-MAPB induced partial release of preloaded [^{3}H]neurotransmitter at the three transporters with rank order of potency hSERT=hNET >hDAT (Table 2, Fig 3D). 5-MAPB, 6-MAPB, 6-APB and 6-EAPB have the furanyl group attached to the phenyl ring in differing configurations (Fig 1E). 5-MAPB and 6-MAPB, with secondary nitrogens, had high nanomolar to low micromolar affinities but much higher potencies for inhibition of uptake, suggesting that these compounds may be substrates. 5-MAPB was fully efficacious in releasing [^{3}H]5-HT from hSERT at nanomolar concentrations, and was partially efficacious at hNET and hDAT at micromolar concentrations (Fig 3E). 6-MAPB had high nanomolar releasing potencies at the transporters, and was fully efficacious at hSERT (Fig 3F). 6-APB, with a primary amine group, had rank order for potency at uptake and release hNET>hDAT>hSERT, however it was a fully efficacious releaser only at hSERT (Fig 3H). 6-EAPB, with an ethyl group on the nitrogen, had rank order of affinity of hDAT>hNET>hSERT, but similar uptake inhibition potencies at hDAT, hNET, and hSERT. 5-MADPB, with a dihydrofuran group, had high selectivity for hSERT over hDAT in binding and uptake assays. It was a fully efficacious hSERT releaser with mid-nanomolar potency, had lower hNET efficacy but higher potency, and much lower hDAT potency and efficacy (Fig 3G). The benzofurans had higher potency at SERT release compared to METH and MCAT (Table 2).

Modeling of drug-receptor interactions

At the binding pocket, hDAT and hNET share 100% sequence similarity, and hSERT has 95.5% similarity with the other two. Due to this high sequence homology, ligands can target all three transporters. The compounds tested here, capable of binding more than one transporter, were analyzed using a structure-based approach to understand the transporter selectivity for selected candidates. In general ligands binding to hSERT, hDAT, and hNET have key pharmacophore features: a protonated nitrogen, an aromatic ring, and a hydrophobic moiety (Fig. 4A). For ligands that bind at the central site (Fig. 4B), the majority of the ligands occupy mainly subsites A and B and some additionally extend to subsite C (Fig 4C). The protonated nitrogen binds subsite A to establish ionic interaction with a conserved aspartate residue (Fig. 4C). The predicted binding poses of the representative ligands matched the experimentally determined paroxetine poses with hSERT (Coleman et al. 2106).

Compounds with differing hDAT/hSERT selectivities were individually modeled. 4-Cl-α-PVP and TH-PVP have one structural variation: 4-Cl-benzene is replaced by tetralin in TH-PVP (Fig 1). The bulky tetralin group binds deeply into subsite B. hSERT residues T-439 and L-443 increase the favorable interaction whereas the hDAT and hNET residues at this position (A-423/S-420 and M-427/M-424) lead to slightly unfavorable interaction (Fig. 5 A&B). Also, extended interaction at subsite C causes the butyl tail in TH-PVP to point downward (Fig. 5C). This position leads to favorable interaction with hSERT V-501, whereas isoleucine in this position causes steric clash with hDAT and hNET. In contrast, the upward positioning of the butyl chain in 4-Cl-α-PVP favorably interacts with hDAT V-152/

hNET V-148, while hSERT I-172 causes steric clash with the butyl tail and decreases affinity. Importantly, the predicted position suggests that the tail location determines selectivity.

Phenethylamine derivatives pentedrone and *N*-propyl PD bind selectively to hDAT and hNET over hSERT (Table 1). The extra carbon present in hSERT I-172 causes steric hindrance to the benzene ring and leads to lower affinity (Fig 5D&E). Benzofuran 5-MAPB prefers hSERT (1.39 μM) over hDAT (2.66 μM) and hNET (3.15 μM). Higher hSERT affinity may be due to increased hydrophobic interaction between the benzofuran benzene ring and hSERT I-172 (Fig 5F), with the furan ring influencing the benzene ring position to increase favorable interaction.

Discussion

First reported more than 30 years ago, a positive relationship exists between affinities of drugs for DAT and potencies of drugs in self-administration (Ritz et al. 1987; Kuhar et al. 1991). Higher affinity and potency at DAT is associated with higher abuse liability and increased activity at SERT is associated with decreased abuse liability (Wee et al. 2005; Wee and Woolverton 2006). The DAT/SERT uptake potency ratio is a predictor of abuse liability (Baumann et al. 2012), and we have applied it to the compounds reported here.

Structure activity studies indicate that modifications to the cathinone molecule can influence *in vitro* and *in vivo* potencies and can aid in predicting whether a compound will be an uptake blocker or a substrate (reviewed in Glennon and Dukat 2017). To increase extracellular neurotransmitter concentrations, uptake blockers are dependent on depolarization-induced release of neurotransmitter, whereas substrates can directly cause an increase by reverse-transport of neurotransmitters (Blough et al. 2014). Primary amines are optimal as substrates, secondary amines are acceptable, but compounds with tertiary amines are uptake blockers. Consistent with this concept, the α-pyrrolidinophenones as a group are uptake blockers, which we and others have reported for many compounds with a 5-membered nitrogen-containing ring (Eshleman et al. 2013; Eshleman et al. 2017; Simmler et al. 2014). The two α-pyrrolidinophenones tested in release assays, TH-PVP and 4-α-Cl-PVP, had no releasing efficacy, consistent with this class of SCs being uptake blockers.

The length of the α-carbon chain of α-pyrrolidinophenones is correlated with uptake inhibition potency (Kolanos et al. 2015; Eshleman et al. 2017). In accordance with these previous findings, 4-Cl-α-PVP (3 carbon tail) had much higher affinities and potencies at DAT, SERT and NET than 4-Cl-α-PPP (1 carbon tail). Similarly, 4-F-α-PHP (4 carbon tail) had higher affinities and potencies at DAT and SERT compared to 4-F-α-PVP (3 carbon tail). Except for 4-Cl-α-PPP and TH-PVP, the DAT/SERT potency ratios range from 83 to 360 for all α-pyrrolidinophenones, which suggests that they have high abuse potential, with the caveat that abuse liability is also dependent on pharmacokinetic parameters such as absorption, metabolism and ability to cross the blood-brain barrier. For many α-pyrrolidinophenones, with similar NE and DA uptake inhibition potencies (Table 1, Figure 2A-D), the *in vivo* stimulant effects will be influenced by blockade of both DAT and NET and subsequent activation of both DA and NE receptors. Similar to the pyrrolidino series, the

length of the α-carbon chain affected potency of pentylone analogs containing the methylenedioxy moiety. Comparing compounds containing tertiary nitrogens, uptake potencies decreased with decreasing carbon tail length for bk-DMBDP, dibutylone and dimethylone.

Para substitutions on the phenyl ring of MCAT, in correlation with their electron-withdrawing capacity, generally decrease DAT potency and may shift selectivity toward SERT (Bonano et al. 2015). In addition, the volume and maximum width of substituents are inversely correlated with DAT selectivity (Sakloth et al. 2015). Our results agree with these observations, although changes in DAT potency were not universal. For example, α-PVP had very high selectivity for DAT compared to SERT, and addition of para-fluoro or para-chloro decreased the selectivity. Pentedrone's DAT selectivity was reduced 18- to 40-fold by addition of a para-chloro or para-methyl, primarily by increasing SERT potency. Similarly, addition of a para-methyl (4-MEAP) to α-EPP decreased DAT selectivity 10-fold by increasing SERT potency. However, addition of para-chloro (4-CEC) to ethylone, a SERT selective compound, did not further decrease DAT selectivity (0.27- to 0.39-fold (Eshleman et al. 2017)). 4-CEC, mexedrone, and ethylone belong to the hybrid DAT blocker-SERT releaser ligand group, which increase extracellular 5-HT more than DA (Blough et al. 2014; Yu et al. 2000; Saha et al. 2015).

MCAT's DAT selectivity was reduced by addition of a meta-methyl (3-MMC), similar to selectivity change when a para-methyl is added to MCAT (mephedrone, 5.2-fold selectivity (Eshleman et al. 2013; Luethi et al. 2018)). No phenyl ring modification increased DAT potency and several increased SERT potency, which could result in compounds with more entactogenic activity while still retaining stimulant properties.

Over the last 5 years benzofuran activity has been investigated on cellular and systems levels. The benzofurans 2-MAPB, 5-MAPB and 5-EAPB, administered orally, elicited 6- to 12-fold increases in extracellular 5-HT levels in mouse striatum (Fuwa et al. 2016), with lower increases in NE and DA. Consistent with these *in vivo* results, we found that all tested benzofurans were fully efficacious releasers *via* SERT and only partial releasers *via* DAT. Using a different methodology (Rickli et al. 2015b) reported lower DAT, SERT and NET potencies of 6-APB and 5-MAPDB for uptake inhibition. Although DAT/SERT ratios were quite different, both Rickli et al. and our results reveal that 5-MAPDB has very low DAT selectivity and may have entactogen activity, while 6-APB has higher DAT/SERT selectivity, but it is still much lower than α-pyrrolidinophenones. 5-MAPB and 6-MAPB (10 μM) displaced [^{125}I]DOI from 5-HT$_{2A,B,C}$ receptors (Shimshoni et al. 2017), and autoradiography with rat brain slices indicates that 5-APB, an analog of 6-APB, displaces both [^{125}I]RTI121 from DAT in the caudate and nucleus accumbens and [^{3}H]ketanserin from 5-HT$_{2A}$ receptors in nucleus accumbens and prefrontal cortex (Dawson et al. 2014), suggesting that benzofuran pharmacology is complex.

Modeling suggested critical pharmacophores (Qing et al. 2014) shared by this set of drugs, and revealed the hDAT/hSERT selectivity reversal between 4-Cl-α-PVP and TH-PVP is due to interactions with hSERT L-443 and T-439. hSERT T-439 also causes steric repulsion of 4'-methyl-α-pyrrolidinopropiophenone (4-MePPP) compared to 4'-methyl-*N*-ethylcathinone

(4-MEC (Saha et al. 2015)). Other residues contributing to selectivity include hSERT I-172 causing steric clash in 4-Cl-α-PVP binding and hDAT V-152/hNET V-148 increasing binding.

The data described here will contribute to decisions about drug scheduling by the United States Drug Enforcement Administration and similar agencies. In Sweden, the use of 6-APB, in addition to other abused compounds, was dramatically affected by scheduling, as daily online posts dropped from 21 to 4, suggesting less interest and use after scheduling (Ledberg 2015). Additionally, these *in vitro* and *in silico* findings may influence structure activity and chemical modeling to better understand drug-transporter interactions and may help to identify specific drug-transporter interfaces.

Acknowledgements

Support Funding for this study was provided by the Department of Justice Drug Enforcement Administration (D-15-OD-0002), Veterans Affairs Merit Review (I01BX002758) and Career Scientist (14S-RCS-006) programs, the Methamphetamine Abuse Research Center (P50 DA018165), and National Institutes of Health/National Institute on Drug Abuse (ADA12013). The contents do not represent the views of the U.S. Department of Veterans Affairs or the United States Government.

Role of funding source DEA project officers contributed to study design and reviewed the manuscript. They had no further role in the collection, analysis and interpretation of data, in the writing of the report, or in the decision to submit the paper for publication.

We thank the OHSU Medicinal Chemistry Core for drug-transporter modeling and analysis.

Reference List

Baumann MH, Ayestas MA Jr., Partilla JS et al. (2012) The designer methcathinone analogs, mephedrone and methylone, are substrates for monoamine transporters in brain tissue. Neuropsychopharmacology 37:1192–1203 [PubMed: 22169943]

Baumann MH, Partilla JS, Lehner KR et al. (2013) Powerful cocaine-like actions of 3,4-methylenedioxypyrovalerone (MDPV), a principal constituent of psychoactive ‘bath salts’ products. Neuropsychopharmacology 38:552–562 [PubMed: 23072836]

Blough BE, Landavazo A, Partilla JS et al. (2014) Hybrid dopamine uptake blocker-serotonin releaser ligands: a new twist on transporter-focused therapeutics. ACS Med Chem Lett 5:623–627 [PubMed: 24944732]

Bonano JS, Banks ML, Kolanos R et al. (2015) Quantitative structure-activity relationship analysis of the pharmacology of para-substituted methcathinone analogues. Br J Pharmacol 172:2433–2444 [PubMed: 25438806]

Cameron K, Kolanos R, Vekariya R, De Felice L, Glennon RA (2013) Mephedrone and methylenedioxypyrovalerone (MDPV), major constituents of “bath salts,” produce opposite effects at the human dopamine transporter. Psychopharmacology (Berl) 227:493–499 [PubMed: 23371489]

Cheng Y, Prusoff WH (1973) Relationship between the inhibition constant (K1) and the concentration of inhibitor which causes 50 per cent inhibition (I50) of an enzymatic reaction. Biochem Pharmacol 22:3099–3108 [PubMed: 4202581]

Coleman JA, Green EM, Gouaux E (2016) X-ray structures and mechanism of the human serotonin transporter. Nature 532:334–339 [PubMed: 27049939]

Dal Cason TA, Young R, Glennon RA (1997) Cathinone: an investigation of several N-alkyl and methylenedioxy-substituted analogs. Pharmacol Biochem Behav 58:1109–1116 [PubMed: 9408221]

Dawson P, Opacka-Juffry J, Moffatt JD et al. (2014) The effects of benzofury (5-APB) on the dopamine transporter and 5-HT2-dependent vasoconstriction in the rat. Prog Neuropsychopharmacol Biol Psychiatry 48:57–63 [PubMed: 24012617]

De Felice LJ, Glennon RA, Negus SS (2014) Synthetic cathinones: chemical phylogeny, physiology, and neuropharmacology. Life Sci 97:20–26 [PubMed: 24231923]

de la Torre R, Farre M, Roset PN et al. (2004) Human pharmacology of MDMA: pharmacokinetics, metabolism, and disposition. Ther Drug Monit 26:137–144 [PubMed: 15228154]

Drug Enforcement Administration (2011) Schedules of controlled substances: temporary placement of three synthetic cathinones in Schedule I. Final Order Fed Regist 76:65371–65375 [PubMed: 22016903]

Drug Enforcement Administration (2017) Schedules of Controlled Substances: Placement of 10 Synthetic Cathinones Into Schedule I. Final rule. Fed Regist 82:12171–12177

Eshleman AJ, Carmolli M, Cumbay M et al. (1999) Characteristics of drug interactions with recombinant biogenic amine transporters expressed in the same cell type. J Pharmacol Exp Ther 289:877–885 [PubMed: 10215666]

Eshleman AJ, Wolfrum KM, Hatfield MG et al. (2013) Substituted methcathinones differ in transporter and receptor interactions. Biochem Pharmacol 85:1803–1815 [PubMed: 23583454]

Eshleman AJ, Wolfrum KM, Reed JF et al. (2017) Structure-Activity Relationships of Substituted Cathinones, with Transporter Binding, Uptake, and Release. J Pharmacol Exp Ther 360:33–47 [PubMed: 27799294]

Friesner RA, Banks JL, Murphy RB et al. (2004) Glide: a new approach for rapid, accurate docking and scoring. 1. Method and assessment of docking accuracy. J Med Chem 47:1739–1749 [PubMed: 15027865]

Friesner RA, Murphy RB, Repasky MP et al. (2006) Extra precision glide: docking and scoring incorporating a model of hydrophobic enclosure for protein-ligand complexes. J Med Chem 49:6177–6196 [PubMed: 17034125]

Fuwa T, Suzuki J, Tanaka T et al. (2016) Novel psychoactive benzofurans strongly increase extracellular serotonin level in mouse corpus striatum. J Toxicol Sci 41:329–337 [PubMed: 27193726]

Gatch MB, Rutledge MA, Forster MJ (2015) Discriminative and locomotor effects of five synthetic cathinones in rats and mice. Psychopharmacology (Berl) 232:1197–1205 [PubMed: 25281225]

Glennon RA, Dukat M (2017) Structure-Activity Relationships of Synthetic Cathinones. Curr Top Behav Neurosci 32:19–47 [PubMed: 27830576]

Hadlock GC, Webb KM, McFadden LM et al. (2011) 4-Methylmethcathinone (mephedrone): neuropharmacological effects of a designer stimulant of abuse. J Pharmacol Exp Ther 339:530–536 [PubMed: 21810934]

Halgren TA, Murphy RB, Friesner RA et al. (2004) Glide: a new approach for rapid, accurate docking and scoring. 2. Enrichment factors in database screening, J Med Chem 47:1750–1759 [PubMed: 15027866]

Hofer KE, Faber K, Muller DM, et al. (2017) Acute Toxicity Associated With the Recreational Use of the Novel Psychoactive Benzofuran N-methyl-5-(2 aminopropyl)benzofuran. Ann Emerg Med 69:79–82 [PubMed: 27156124]

Iversen L, Gibbons S, Treble R et al. (2013) Neurochemical profiles of some novel psychoactive substances. Eur J Pharmacol 700:147–151 [PubMed: 23261499]

King LA, Corkery JM (2018) An index of fatal toxicity for new psychoactive substances. J Psychopharmacol 32:793–801 [PubMed: 29482434]

Kolanos R, Sakloth F, Jain AD et al. (2015) Structural Modification of the Designer Stimulant alpha-Pyrrolidinovalerophenone (alpha-PVP) Influences Potency at Dopamine Transporters. ACS Chem Neurosci 6:1726–1731 [PubMed: 26217965]

Krotulski AJ, Mohr LA, Papsun DM, Logan BK (2018) Dibutylone (bk-DMBDB): Intoxications, Quantitative Confirmations and Metabolism in Authentic Biological Specimens. J Anal Toxicol 42:437–445 [PubMed: 29554274]

Kuhar MJ, Ritz MC, Boja JW (1991) The dopamine hypothesis of the reinforcing properties of cocaine. Trends Neurosci 14:299–302 [PubMed: 1719677]

Ledberg A (2015) The interest in eight new psychoactive substances before and after scheduling. Drug Alcohol Depend 152:73–78 [PubMed: 25981311]

Lopez-Arnau R, Martinez-Clemente J, Pubill D et al. (2012) Comparative neuropharmacology of three psychostimulant cathinone derivatives: butylone, mephedrone and methylone. Br J Pharmacol 167:407–420 [PubMed: 22509960]

Luethi D, Kolaczynska KE, Docci L et al. (2018) Pharmacological profile of mephedrone analogs and related new psychoactive substances. Neuropharmacology 134:4–12 [PubMed: 28755886]

Marusich JA, Antonazzo KR, Wiley JL et al. (2014) Pharmacology of novel synthetic stimulants structurally related to the “bath salts” constituent 3,4-methylenedioxypyrovalerone (MDPV). Neuropharmacology 87:206–213 [PubMed: 24594476]

McLaughlin G, Morris N, Kavanagh PV et al. (2017) Synthesis, characterization and monoamine transporter activity of the new psychoactive substance mexedrone and its N-methoxy positional isomer, N-methoxymephedrone. Drug Test Anal 9:358–368 [PubMed: 27524685]

Meltzer PC, Butler D, Deschamps JR, Madras BK (2006) 1-(4-Methylphenyl)-2-pyrrolidin-1-yl-pentan-1-one (Pyrovalerone) analogues: a promising class of monoamine uptake inhibitors. J Med Chem 49:1420–1432 [PubMed: 16480278]

Monte AP, Marona-Lewicka D, Cozzi NV, Nichols DE (1993) Synthesis and pharmacological examination of benzofuran, indan, and tetralin analogues of 3,4-(methylenedioxy)amphetamine. J Med Chem 36:3700–3706 [PubMed: 8246240]

Qing X, Lee XY, De Raeymaecker J, Tame J et al. (2014) Pharmacophore modeling: advances, limitations, and current utility in drug discovery. J Receptor Ligand Channel Res 7:81–92

Rickli A, Hoener MC, Liechti ME (2015a) Monoamine transporter and receptor interaction profiles of novel psychoactive substances: para-halogenated amphetamines and pyrovalerone cathinones. Eur Neuropsychopharmacol 25:365–376 [PubMed: 25624004]

Rickli A, Kopf S, Hoener MC, Liechti ME (2015b) Pharmacological profile of novel psychoactive benzofurans. Br J Pharmacol 172:3412–3425 [PubMed: 25765500]

Ritz MC, Lamb RJ, Goldberg SR, Kuhar MJ (1987) Cocaine receptors on dopamine transporters are related to self-administration of cocaine. Science 237:1219–1223 [PubMed: 2820058]

Roberts L, Ford L, Patel N et al. (2017) 11 analytically confirmed cases of mexedrone use among polydrug users. Clin Toxicol (Phila) 55:181–186 [PubMed: 28075189]

Saha K, Partilla JS, Lehner KR et al. (2015) ‘Second-generation’ mephedrone analogs, 4-MEC and 4-MePPP, differentially affect monoamine transporter function. Neuropsychopharmacology 40:1321–1331 [PubMed: 25502630]

Sahai MA, Davidson C, Khelashvili G et al. (2017) Combined in vitro and in silico approaches to the assessment of stimulant properties of novel psychoactive substances - The case of the benzofuran 5-MAPB. Prog Neuropsychopharmacol Biol Psychiatry 75:1–9 [PubMed: 27890676]

Sakloth F, Kolanos R, Mosier PD et al. (2015) Steric parameters, molecular modeling and hydropathic interaction analysis of the pharmacology of para-substituted methcathinone analogues. Br J Pharmacol 172:2210–2218 [PubMed: 25522019]

Sali A, Blundell TL (1993) Comparative protein modelling by satisfaction of spatial restraints. J Mol Biol 234:779–815 [PubMed: 8254673]

Sandtner W, Stockner T, Hasenhuetl PS et al. (2016) Binding Mode Selection Determines the Action of Ecstasy Homologs at Monoamine Transporters. Mol Pharmacol 89:165–175 [PubMed: 26519222]

Schindler CW, Thorndike EB, Goldberg SR et al. (2016) Reinforcing and neurochemical effects of the “bath salts” constituents 3,4-methylenedioxypyrovalerone (MDPV) and 3,4-methylenedioxy-N-methylcathinone (methylone) in male rats. Psychopharmacology (Berl) 233:1981–1990 [PubMed: 26319160]

Shen MY, Sali A (2006) Statistical potential for assessment and prediction of protein structures. Protein Sci 15:2507–2524 [PubMed: 17075131]

Sherman W, Day T, Jacobson MP et al. (2006) Novel procedure for modeling ligand/receptor induced fit effects. J Med Chem 49:534–553 [PubMed: 16420040]

Shimshoni JA, Winkler I, Golan E, Nutt D (2017) Neurochemical binding profiles of novel indole and benzofuran MDMA analogues. Naunyn Schmiedebergs Arch Pharmacol 390:15–24 [PubMed: 27650729]

Simmler LD, Liechti ME (2017) Interactions of Cathinone NPS with Human Transporters and Receptors in Transfected Cells. Curr Top Behav Neurosci 32:49–72 [PubMed: 27272068]

Simmler LD, Liechti ME (2018) Pharmacology of MDMA- and Amphetamine-Like New Psychoactive Substances In: Handbook of Experimental Pharmacology. Springer, Berlin, Heidelberg

Simmler LD, Rickli A, Hoener MC, Liechti ME (2014) Monoamine transporter and receptor interaction profiles of a new series of designer cathinones. Neuropharmacology 79:152–160 [PubMed: 24275046]

Staeheli SN, Boxler MI, Oestreich A et al. (2017) Postmortem distribution and redistribution of MDAI and 2-MAPB in blood and alternative matrices. Forensic Sci Int 279:83–87 [PubMed: 28850871]

Tettey JNA, Crean C, Ifeagwu SC, Raithelhuber M (2018) Emergence, Diversity, and Control of New Psychoactive Substances: A Global Perspective In: Handbook of Experimental Pharmacology. Springer, Berlin, Heidelberg

Tyrkko E, Andersson M, Kronstrand R (2016) The Toxicology of New Psychoactive Substances: Synthetic Cathinones and Phenylethylamines. Ther Drug Monit 38:190–216 [PubMed: 26587869]

Uchiyama N, Matsuda S, Kawamura M et al. (2014) Characterization of four new designer drugs, 5-chloro-NNEI, NNEI indazole analog, alpha-PHPP and alpha-POP, with 11 newly distributed designer drugs in illegal products. Forensic Sci Int 243:1–13 [PubMed: 24769262]

Webb B, Sali A (2017) Protein Structure Modeling with MODELLER. Methods Mol Biol 1654: 39–54 [PubMed: 28986782]

Wee S, Anderson KG, Baumann MH et al. (2005) Relationship between the serotonergic activity and reinforcing effects of a series of amphetamine analogs. J Pharmacol Exp Ther 313:848–854 [PubMed: 15677348]

Wee S, Woolverton WL (2006) Self-administration of mixtures of fenfluramine and amphetamine by rhesus monkeys. Pharmacol Biochem Behav 84: 337–343 [PubMed: 16828855]

Welter-Luedeke J, Maurer HH (2016) New Psychoactive Substances: Chemistry, Pharmacology, Metabolism, and Detectability of Amphetamine Derivatives With Modified Ring Systems. Ther Drug Monit 38:4–11 [PubMed: 26327309]

Yu H, Rothman RB, Dersch CM et al. (2000) Uptake and release effects of diethylpropion and its metabolites with biogenic amine transporters. Bioorg Med Chem 8:2689–2692 [PubMed: 11131159]

A. α-pyrrolidino substituted cathinones

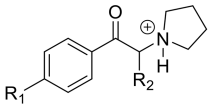

Drug	R_1	R_2
α-PVP	H	$(CH_2)_2CH_3$
4-Cl-α-PPP	Cl	CH_3
4-F-α-PVP	F	$(CH_2)_2CH_3$
4-Cl-α-PVP	Cl	$(CH_2)_2CH_3$
4-F-α-PHP	F	$(CH_2)_3CH_3$
4-Me-α-PHP	CH_3	$(CH_2)_3CH_3$
PV9	H	$(CH_2)_5CH_3$

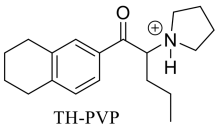

TH-PVP

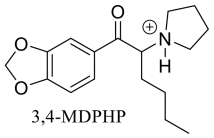

3,4-MDPHP

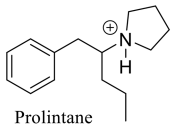

Prolintane

B. Pentedrone analogs

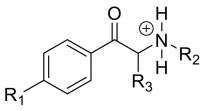

Drug	R_1	R_2	R_3
Pentedrone	H	CH_3	$(CH_2)_2CH_3$
4-MPD	CH_3	H	$(CH_2)_2CH_3$
4-CPD	Cl	H	$(CH_2)_2CH_3$
α-EPP	H	CH_2CH_3	$(CH_2)_2CH_3$
N-propyl PD	H	$(CH_2)_2CH_3$	$(CH_2)_2CH_3$
4-MEAP	CH_3	CH_2CH_3	$(CH_2)_2CH_3$
N-Et Hexedrone	H	CH_2CH_3	$(CH_2)_3CH_3$

C. Pentylone analogs

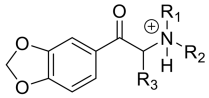

Drug	R_1	R_2	R_3
Pentylone	H	CH_3	$(CH_2)_2CH_3$
bk-DMBDP	CH_3	CH_3	$(CH_2)_2CH_3$
N-Et Pentylone	H	CH_2CH_3	$(CH_2)_2CH_3$
Dibutylone	CH_3	CH_3	CH_2CH_3
Dimethylone	CH_3	CH_3	CH_3
PRONE	H	$(CH_2)_2CH_3$	CH_3

D. Other MCAT analogs

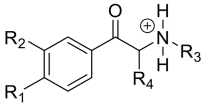

Drug	R_1	R_2	R_3	R_4
MCAT	H	H	CH_3	CH_3
3-MMC	H	CH_3	CH_3	CH_3
4-CEC	Cl	H	CH_2CH_3	CH_3
Mexedrone	CH_3	H	CH_3	$CH_2O\ CH_3$

E. Benzofurans

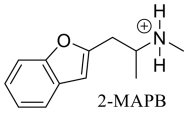

2-MAPB

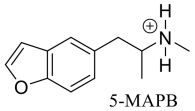

5-MAPB

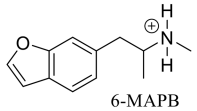

6-MAPB

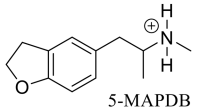

5-MAPDB

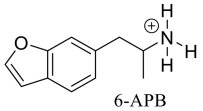

6-APB

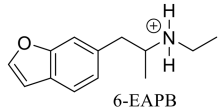

6-EAPB

F. METH and MDMA

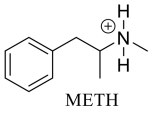

METH

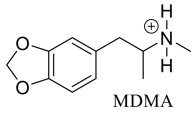

MDMA

33

Figure 1.

Structures of substituted cathinones, benzofurans, prolintane, METH and MDMA at physiological pH.

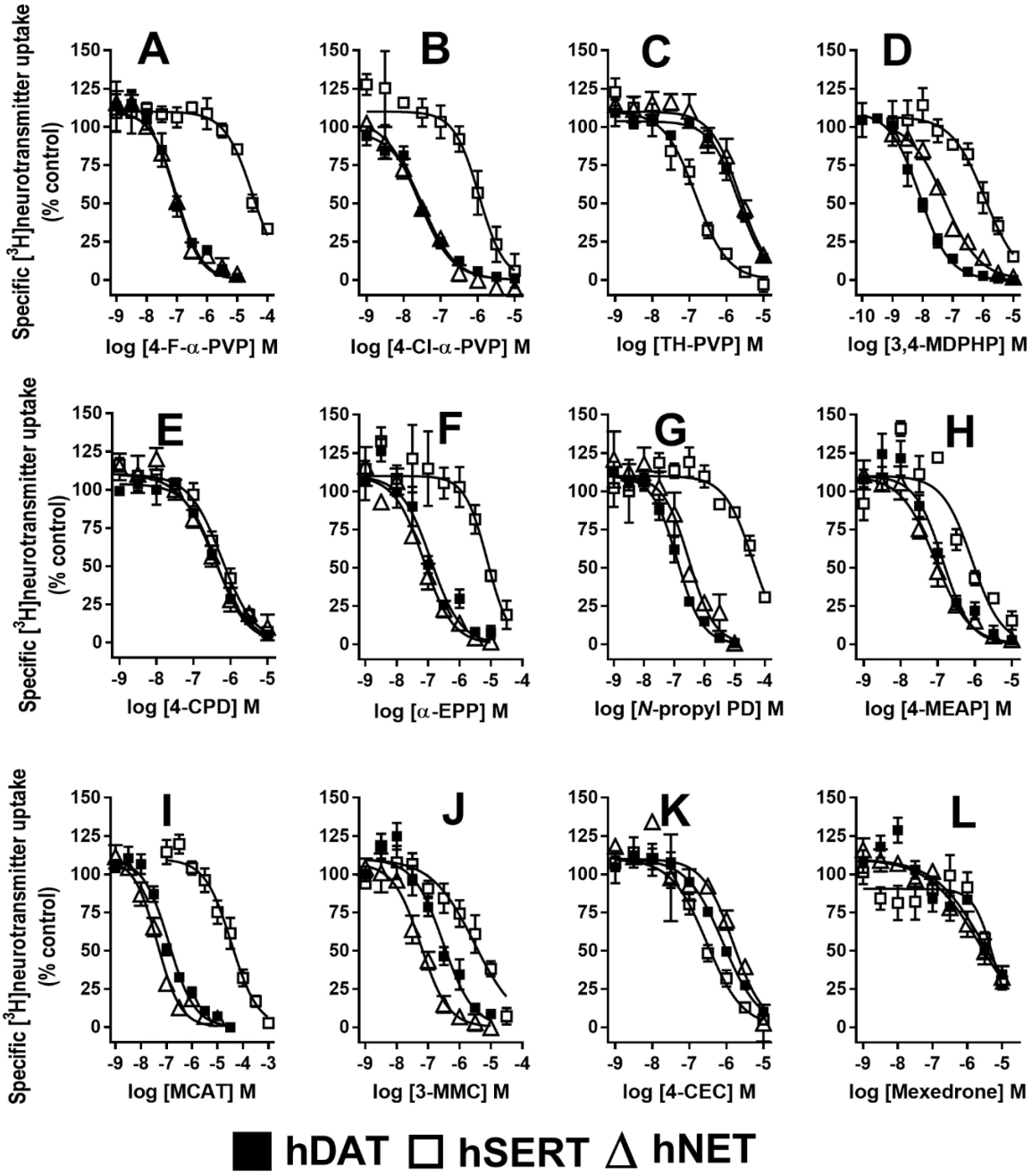

Figure 2.

Concentration-response curves of 12 substituted cathinones for inhibition of [^{3}H]DA uptake by hDAT, [^{3}H]5-HT uptake by hSERT and [^{3}H]NE uptake by hNET. (A) 4-F-α-PVP, (B), 4-Cl-α-PVP, (C) TH-PVP, (D) 3,4-MDPHP, (E) 4-CPD, (F) α-EPP, (G) *N*-propyl PD, (H) 4-MEAP, (I) MCAT, (J) 3-MMC, (K) 4-CEC and (L)Mexedrone. Data are the mean and S.E.M. of three or more experiments, each conducted in duplicate.

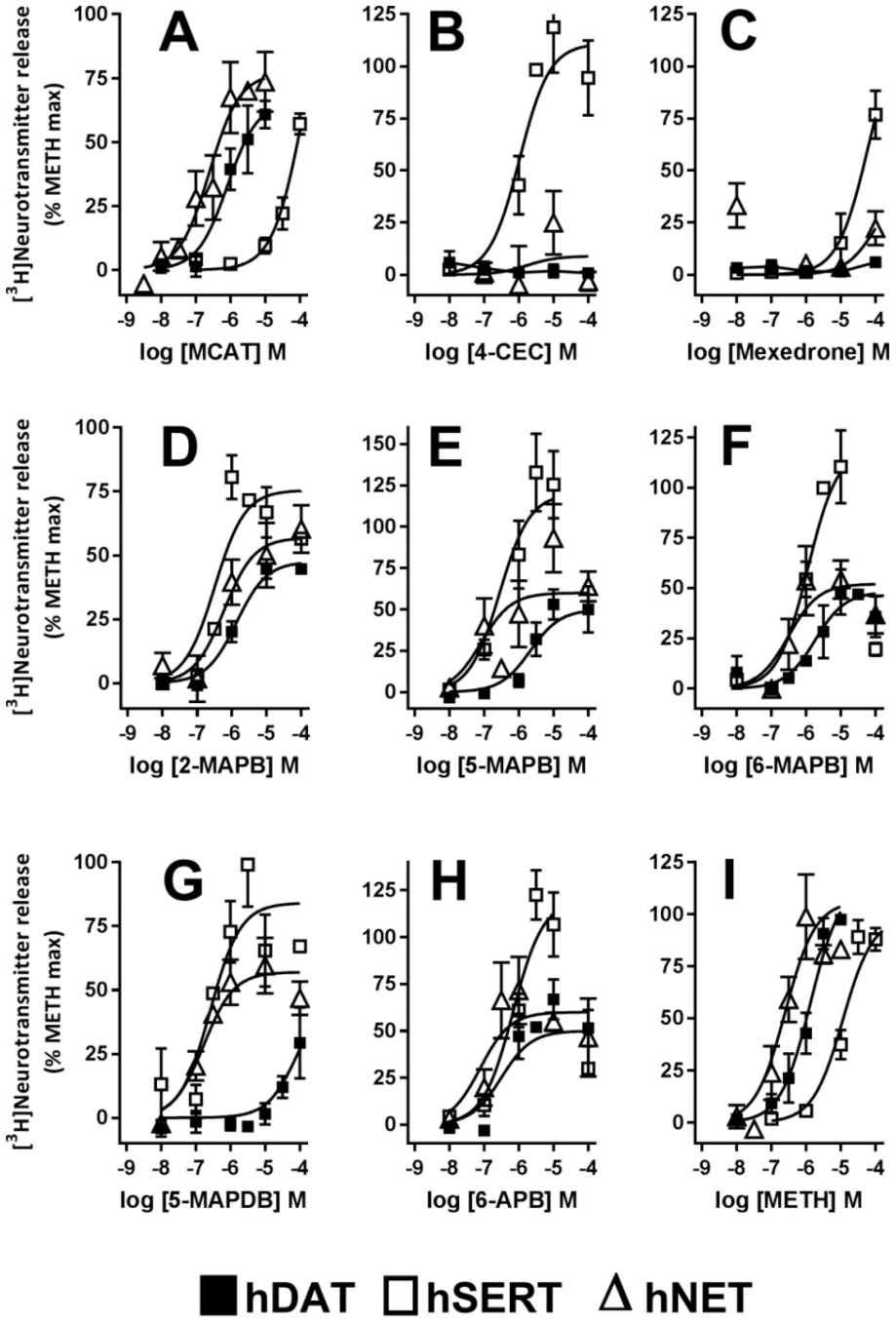

Figure 3.

Concentration-response curves for [^{3}H]neurotransmitter release by METH, MCAT, and 7 substituted cathinones and benzofurans. (A) MCAT, (B) 4-CEC, (C) Mexedrone, (D) 2-MAPB, (E) 5-MAPB, (F) 6-MAPB, (G) 5-MAPDB, (H) 6-APB and (I) METH. The AUC for each drug concentration was normalized to the maximal METH effect. hDAT: [^{3}H]DA release. hSERT: [^{3}H]5-HT release. hNET: [^{3}H]NE release. Data are the mean and S.E.M. of three or more experiments, except when a drug had no releasing efficacy, when data are the mean and range of two experiments.

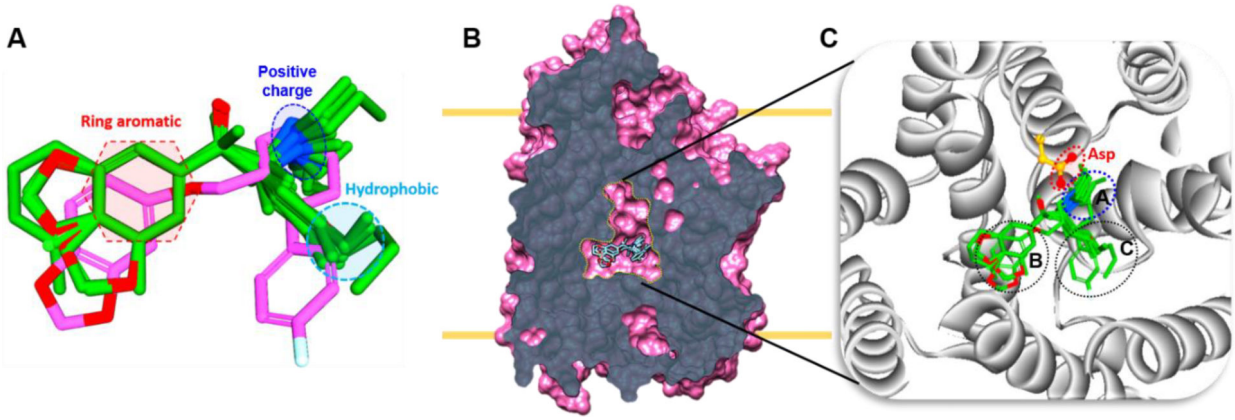

Figure 4.

Alignment of all ligands in the binding pocket. A. Ligand alignment based on the paroxetine binding pose derived from hSERT crystal structure (PDB: 5I6X). Key pharmacophore features such as positive charge, aromatic ring and hydrophobic are shown in the dotted lines. B. Slab view of hSERT and the central site showing aligned ligands. C. An enlarged view of central site and plausible ligand binding poses, dotted lines indicate subsites A, B, and C.

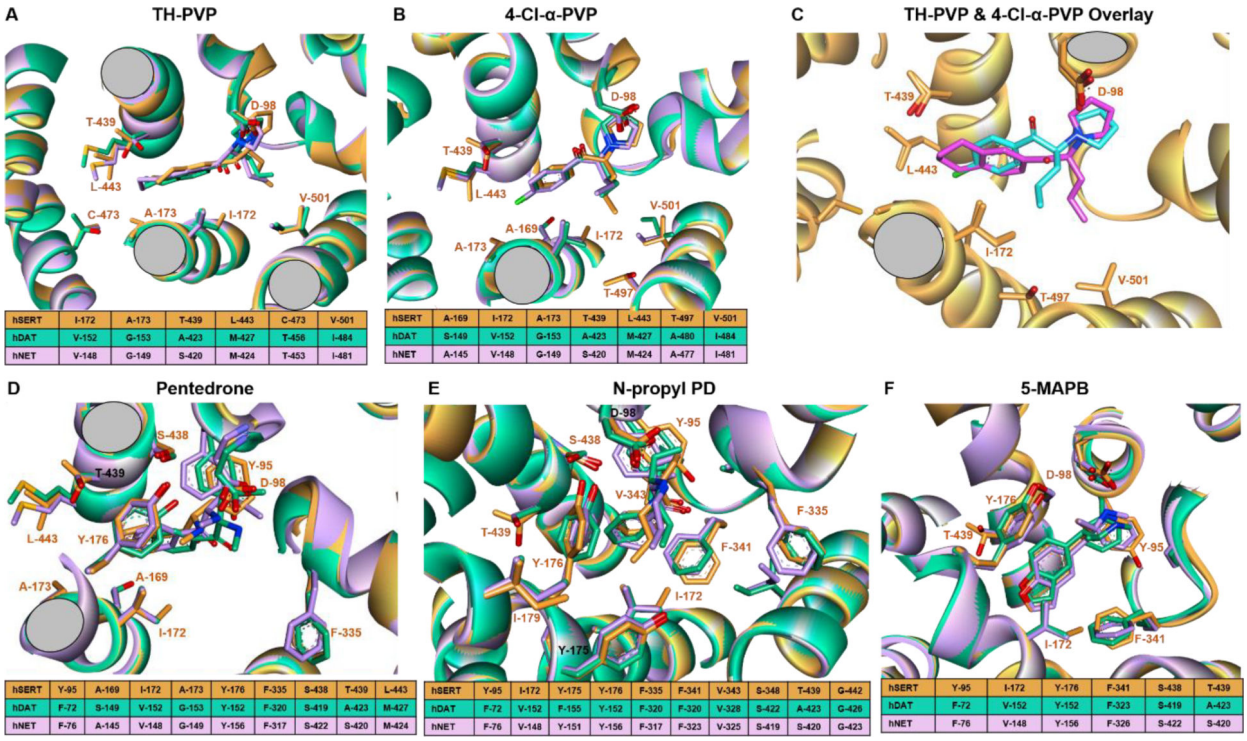

Figure 5.

Modeling of representative ligands. A) Superimposition of predicted docking poses of TH-PVP against the three transporters, hSERT residues are labeled and indicated with orange stick and carton, hDAT and hNET are represented in green and pink colors, respectively. The sequence comparison table in the bottom shows aligned sequences of the transporters in the same position. The color code is the same for all the panels except for panel C. B) Predicted pose of 4-Cl-α-PVP. C) Overlay of the predicted binding poses 4-Cl-α-PVP (blue stick) and TH-PVP (pink stick), and protein in orange. The selectivity is caused by the different position of the butyl tail of each ligand. For clarity, only hSERT is shown. D) Pentedrone E) *N*-propyl PD F) 5-MAPB.

Psychopharmacology (Berl). Author manuscript; available in PMC 2020 March 01.

Table 1.

Affinity and potency of substituted cathinones, benzofurans, prolintane and standard compounds at hDAT, hSERT and hNET.

	Inhibition of [^{125}I]RTI-55 binding Ki ± sem (μM) (n)			Inhibition of [^{3}H]neurotransmitter uptake IC_{50} ± sem (μM) (n)			Ratio
Drug	**hDAT**	**hSERT**	**hNET**	**hDAT [^{3}H]DA**	**hSERT [^{3}H]5-HT**	**hNET [^{3}H]NE**	**DAT/SERT**
α- pyrrolidinophenones							
α-PVP[a]	0.0222 ± 0.0053 (7)	68 ± 18	0.122 ± 0.029 (3)	0.0197 ± 0.0048 (5)	57 ± 14 (3)	0.046 ± 0.018 (5)	2900
4-Cl-α-PPP	1.30 ± 0.45 (5)	12.7 ± 3.2 (3)	3.58± 0.92 (5)	0.73 ± 0.13 (4)	6.4 ± 1.5 (3)	1.42 ± 0.38 (5)	8.8
4-F-α-PVP	0.376 ± 0.070 (5)	14.7 ± 1.6 (6)	1.10 ± 0.10 (4)	0.119 ± 0.025 (3)	42.5 ± 6.0 (4)	0.118 ± 0.017 (3)	360
4-Cl-α-PVP	0.061 ± 0.015 (4)	2.02 ± 0.19 (4)	0.281 ± 0.016 (4)	0.0248 ± 0.0014 (3)	2.07 ± 0.33 (3)	0.0291 ± 0.0067 (3)	83
4-F-α-PHP	0.122 ± 0.027 (6)	8.01 ± 0.84 (5)	1.73 ± 0.25 (4)	0.0382 ± 0.0044 (4)	9.11 ± 0.54 (4)	0.218 ± 0.029 (3)	240
4-Me-α-PHP	0.0230 ± 0.0062 (4)	4.78 ± 0.26 (3)	0.75 ± 0.16 (4)	0.0132 ± 0.0036 (4)	1.58 ± 0.40 (5)	0.042 ± 0.011 (4)	120
3,4-MDPHP	0.0192 ± 0.0051 (3)	2.43 ± 0.51 (3)	0.935 ± 0.093 (3)	0.0084 ± 0.0022 (3)	1.34 ± 0.41 (3)	0.047 ± 0.010 (3)	160
PV9	0.0180 ± 0.0037 (5)	2.86 ± 0.43 (3)	0.468 ± 0.033 (3)	0.0502 ± 0.0066 (3)	>7.4 μM	0.0304 ± 0.0.0059 (3)	>150
TH-PVP	3.09 ± 0.30 (4)	0.131 ± 0.028 (3)	6.95 ± 0.34 (3)	2.40 ± 0.11 (3)	0.208 ± 047 (5)	2.129 ± 0.081 (3)	0.087
Other cathinones							
Pentedrone[a]	0.339 ± 0.098 (7)	16.4 ± 4.6 (3)	1.95 ± 0.56 (5)	0.1762 ± 0.0089 (3)	9.0 ± 2.3 (3)	0.239 ± 0.067 (3)	51
4-MPD	1.45 ± 0.31 (3)	6.2 ± 1.4 (6)	3.39 ± 0.48 (3)	0.188 ± 0.03 (3)	0.532 ± 0.016 (3)	0.307 ± 0.061 (3)	2.8
4-CPD	1.62 ± 0.40 (4)	3.85 ± 0.55 (3)	4.54 ± 0.89 (3)	0.486 ± 0.067 (3)	0.61 ± 0.15 (3)	0.47 ± 0.14 (4)	1.3
α-EPP	0.182 ± 0.022 (4)	8.4 ± 2.1 (5)	0.70 ± 0.18 (3)	0.165 ± 0.043(3)	10.5 ± 2.0 (3)	0.101 ± 0.024 (3)	64
N-propyl pentedrone	0.389 ± 0.067 (3)	>30 μM (3)	3.76 ± 0.82 (3)	0.127 ± 0.023 (3)	42.0 ± 4.9 (4)	0.306 ± 0.079 (3)	330
4-MEAP	0.123 ± 0.026 (3)	0.765 ± 0.073 (3)	0.576 ± 0.085 (3)	0.179 ± 0.034 (3)	1.14 ± 0.12 (3)	0.083 ± 0.018 (5)	6.4
N-Et-Hexedrone	0.171 ± 0.038 (3)	11.4 ± 1.8 (3)	1.259 ± 0.043 (3)	0.0467 ± 0.0040 (3)	4.88 ± 0.47 (3)	0.0978 ± 0.0083 (3)	100
Pentylonea	0.3942 ± 0.0040 (3)	3.38 ± 0.52 (4)	8.19 ± 0.57 (3)	0.167 ± 0.037 (3)	0.81 ± 0.14 (4)	0.65 ± 0.16 (3)	4.9
N-Et pentylone	0.102 ± 0.015 (4)	0.893 ± 0.080 (3)	2.38 ± 0.62 (3)	0.0549 ± 0.0073 (3)	0.46 ± 0.12 (4)	0.114 ± 0.029 (6)	8.4
bk-DMBDP	0.354 ± 0.073 (3)	2.27 ± 0.30 (3)	2.00 ± 0.14 (3)	0.233 ± 0.066 (3)	2.57 ± 0.55 (5)	0.212 ± 0.068 (4)	11
Dibutylone	0.581 ± 0.076 (4)	>10 μM (2)	8.4 ± 2.1 (3)	0.302 ± 0.013 (3)	>9.7 μM (3)	0.923 ± 0.044 (3)	>32
Dimethylone	4.21 ± 0.27 (3)	>10 μM (3)	>10 μM (2)	2.22 ± 0.36 (3)	>9.2 μM (3)	4.20 ± 0.88 (4)	>4.1
PRONE	6.8 ± 1.9 (3)	13.3 ± 1.0 (3)	22.5 ± 8.5 (3)	2.38 ± 0.46 (3)	2.25 ± 0.35 (3)	6.04 ± 0.89 (3)	0.95
MCAT	7.52 ± 0.99 (17)	312 a±34 (18)	5.96 ± 0.61 (17)	0.225 ± 0.038 (23)	29.4 ± 6.7 (22)	0.0452 ± 0.0042 (19)	130

	Inhibition of [^{125}I]RTI-55 binding Ki ± sem (μM) (n)			Inhibition of [^{3}H]neurotransmitter uptake IC_{50} ± sem (μM) (n)			Ratio
Drug	**hDAT**	**hSERT**	**hNET**	**hDAT [^{3}H]DA**	**hSERT [^{3}H]5-HT**	**hNET [^{3}H]NE**	**DAT/SERT**
3-MMC	6.33 ± 0.72 (3)	7.9 ± 1.8 (4)	2.85 ± 0.72 (4)	0.433 ± 0.089 (3)	4.5 ± 1.3 (5)	0.084 ± 0.023 (5)	10
4-CEC	4.17 ± 0.53 (3)	7.9 ± 1.2 (3)	16.3 ± 5.7 (5)	0.931 ± 0.080 (3)	0.36 ± 0.10 (5)	1.72 ± 0.24 (3)	0.39
Mexedrone	8.39 ± 0.54 (3)	22.2 ± 6.2 (3)	>27.6 μM (2)	2.75 ± 0.22 (3)	5.4 ± 1.2 (3)	3.19 ± 0.98 (5)	2.0
Benzofurans							
2-MAPB	1.63 ± 0.44 (3)	2.97 ± 0.18 (3)	1.99 ± 0.22 (3)	0.233 ± 0.061 (5)	0.693 ± 0.068 (3)	0.0393 ± 0.0052 (3)	3.0
5-MAPB	2.66 ± 0.61 (3)	1.39 ± 0.33 (3)	3.15 ± 0.27 (3)	0.099 ± 0.010 (3)	0.137 ± 0.024 (3)	0.073 ± 0.018 (3)	1.4
6-MAPB	0.5993 ± 0.0099 (3)	3.85 ± 0.66 (3)	1.48 ± 0.27 (3)	0.052 ± 0.017 (4)	0.496 ± 0.074 (3)	0.0331 ± 0.0020 (3)	9.5
6-APB	1.04 ± 0.16 (4)	2.75 ± 0.62 (3)	2.45 ± 0.20 (4)	0.121 ± 0.022 (4)	0.290 ± 0.062 (4)	0.0198 ± 0.0044 (4)	2.4
6-EAPB	0.089 ± 0.022 (3)	1.31 ± 0.25 (3)	0.772 ± 0.044 (3)	0.051 ± 0.012 (4)	0.0719 ± 0.0094 (5)	0.042 ± 0.014 (4)	1.4
5-MAPDB	>30 μM (3)	8.8 ± 1.7 (4)	>30 μM (3)	2.79 ± 0.80 (3)	0.113 ± 0.030 (4)	0.56 ± 0.18 (3)	0.041
Other noncathinones							
Prolintane	0.219 ± 0.019 (3)	2.52 ± 0.33 (3)	0.56 ± 0.19 (3)	0.100 ± 0.021 (3)	1.11 ± 0.35 (6)	0.0460 ± 0.0068 (3)	11
METH	4.41 ± 0.43 (20)	150 ± 17 (20)	2.51 ± 0.24 (16)	0.097 ± 0.013 (21)	9.3 ± 1.1 (18)	0.0258 ± 0.0030 (19)	96
MDMA	31.0 ± 4.9 (6)	17.5 ± 3.3 (6)	15.8 ± 4.1 (7)	0.479 ± 0.070 (4)	0.118 ± 0.019 (4)	0.63 ± 0.14 (3)	0.25
Cocaine	0.495 ± 0.049 (22)	0.495 ± 0.034 (20)	1.95 ± 0.15 (18)	0.425 ± 0.036 (23)	0.364 ± 0.040 (24)	0.382 ± 0.037 (23)	0.86

(n) Number of independent experiments conducted in duplicate.

Data are normalized to specific binding or specific uptake in the absence of drugs. Drugs were tested in binding and uptake assays at concentrations ranging from 1 nM to 10 μM, 100 μM or 1 mM.

[a]Data from (Eshleman et al. 2017), with permission.

Table 2:

Potency and efficacy of substituted cathinones and standard compounds to release preloaded [^{3}H]neurotransmitter from HEK-hDAT, HEK-hSERT and HEK-hNET cells.

Drug	Drug-induced release of [^{3}H]neurotransmitter EC_{50} ± sem (μM) (n) % maximum release ± sem*		
	hDAT [^{3}H]DA	hSERT [^{3}H]5-HT	hNET [^{3}H]NE
Substituted cathinones			
MCAT	1.57 ± 0.48 (8)	54 ± 17 (3)	0.40 ± 0.12 (5)
	79.0 ± 3.2%	65.0 ± 0.6%	75 ± 10%
4-Cl-α-PVP	>10 μM (2)	>10 μM (2)	>10 μM (2)
	<1%	<1%	9.4 ± 6.0%
TH-PVP	>10 μM (2)	>10 μM (2)	>10 μM (2)
	<1%	<1%	<1%
N-Et pentylone	>10 μM (2)	>10 μM (2)	>6,700 (3)
	<1%	7.2 ± 1.4%	15.6 ± 8.4%
Dimethylone	>10 μM (2)	>10 μM (2)	>10 μM (2)
	<1%	<1%	9.9 ± 2.2%
4-CEC	>100 μM (2)	0.78 ± 0.17 (3) 92	>100 μM (2)
	1.17 ± 0.05%	± 14%	5.9 ± 2.5%
Mexedrone	>100 μM (2)	26.1 ± 9.3 (3)	>61 μM (2)
	3.04 ± 0.61%	84 ± 13%	12.5 ± 3.1%
Benzofurans			
2-MAPB	2.08 ± 0.31 (3)	0.35 ± 0.13 (3)	0.45 ± 0.12 (4)
	48.0 ± 2.6%	77.3 ± 5.3%	63 ± 10%
5-MAPB	2.61 ± 0.68 (3)	0.40 ± 0.14 (3)	0.58 ± 0.21 (7)
	53.8 ± 6.6%	104.3 ± 5.7%	89.0 ± 8.0%
6-MAPB	0.86 ± 0.12 (4)	0.91 ± 0.24 (3)	0.64 ± 0.21 (5)
	40.6 ± 8.7%	107.0 ± 2.3%	60 ± 11%
6-APB	0.582 ± 0.088 (3)	0.85 ± 0.15 (3)	0.051 ± 0.012 (7)
	68.2 ± 9.0%	119 ± 16%	69 ± 12%
5-MAPDB	34.7 ± 9.6 (4)	0.340 ± 0.035 (4)	0.84 ± 0.31 (9)
	32 ± 13%	95.7 ± 8.9%	64.2 ± 4.7%
Non-cathinones			
METH	1.20 ± 0.35 (6)	14.5 ± 4.2 (6)	0.255 ± 0.078 (3)
	106.7 ± 2.3	101.8 ± 3.1%	107.5 ± 8.7%
MDMA[a]	7.5 ± 2.3 (10)	1.10 ± 0.29 (9)	0.360 ± 0.092 (7)
	94 ± 10%	85.1 ± 7.8%	147 ± 15%

(n) Number of independent experiments.

[*] Maximum release is defined as the maximum release (maximal AUC) induced by METH (1 or 10 μM, hDAT; 0.3 or 1 μM, hNET; 0.3–1 mM, hSERT) for each experiment. When the data could not be fit by nonlinear regression (EC_{50} > 10 or 100 μM), the maximum release is the average of release at the 3 highest concentrations tested.

[a] Data from (Eshleman et al. 2017), with permission.